J. of Basic Sciences, Cheju Nat'l Univ.
18(2), 105~113, 2005

기초과학연구 제주대학교
18(2), 105~113, 2005

Simulation on the Neuronal Parabolic Bursting of abdominal ganglion of *Aplysia juliana*

Nam Gyu Hyun, Yong-Joo Kim, and Won-Taek Kim*
Department of Physics, Cheju National University. Jeju 690-756,
**Department of Life Science, Cheju National University, Jeju 690-756.*

This paper traced the partial character in the physiology of the abdominal ganglion of *Aplysia juliana* commonly found in eastern Asian pacific coast. In addition the simulation of the bursting activity of a neuron in *Aplysia juliana* recorded at the neurobiophysics laboratory in Cheju National University. But J. Rinzel and Y. S. Lee have showed that parabolic R-15 type bursts can be generated with a calcium-activated potassium channel. The experimentally measured data have been compared with the result of simulation by using Mathematica program and their model was appropriate for the simulation.

I. INTRODUCTION

Many of the neurons of *Aplysia* abdominal ganglion display spontaneous activity in one of two common forms: a more or less regular firing pattern known as "beating", or clusters of action potentials separated by relatively long period of hyperpolarization known as "bursting". [1]

The R15 cell in the abdominal ganglion of *Aplysia* has been used extensively to gain insights into the biophysical mechanisms underlying endogeneous bursting activity in nerve cells: [2] It fires membrane action potentials in bursts, consisting of regular trains of action potentials separated by silent periods during which the membrane potential is hyperpolarized. The burst rhythm persists for many hours with constant frequency. [3] In R15, the spike frequency increases until the midburst and then decreases again (i.e., a parabolic burst). And a number of Hodgkin-Huxley equivalent circuit models of R15 have been developed that simulate aspects of the activity of R15. [1–9]

In this paper, we partially charactered physiology of the abdominal ganglion of *Aplysia juliana*, which are commonly found in Eastern Asian Pacific coastal lines, [10], and simulated the bursting activity of a neuron in *Aplysia juliana* recorded at the neurobiophysics Lab in Cheju National University by using Mathematica program for evaluation.

II. MATERIALS AND METHODS

Animals.

Aplysia juliana were purchased from professional sea-divers in Jeju. *Aplysia juliana* looked similar to *Aplysia kurodai* in body color pattern, it did not have inking behavior. Animals were maintained in a recircular sea water bath at $17°C$.[10]

III. ELECTROPHYSIOLOGY

The membrane potential of neurons in the intact abdominal ganglia was recorded by using Nueroprove Amplifier(Model 1600) with microelectrodes filled with $3MKCl$. The Impedance of microelectrodes ranged from 5 to 15 $M\Omega$. Data was registered by using A/D converter with LabVIEW.[10]

IV. EXPERIMENTAL RESULTS

The Nervous system of *Aplysia juliana* can be divided into two parts, the head ganglia and the abdominal ganglion. The circumesophageal ring forms around the esophagus and consists of eight head ganglia: two fused cerebrals, two pedals, two plurals, and two buccals. They are arrayed in symmetrical pairs with nerve connectives. They are known to be mainly involved in the somatic functions of controlling movements of the musculature. The viceral connectives between the plural and abdominal ganglia are long and abdominal ganglion lies some distance behind the central ganglia. The asymmetric abdominal ganglion controls many visceral functions such as reproductive, excretory, circulatory, and respiratory functions. The ganglion is

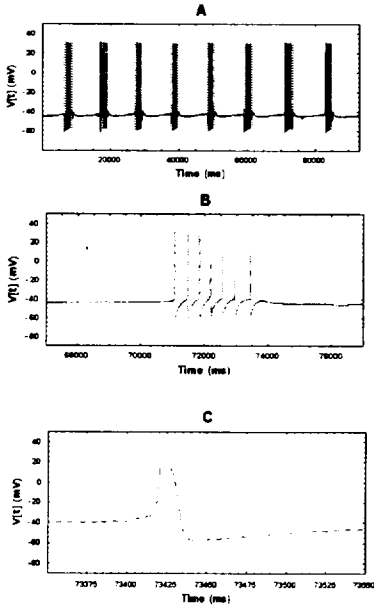

FIG. 1: A: A bursting pattern recorded from the abdominal ganglion of *Aplysia juliana* at the neurobiophysics laboratory in CNU. B,C: The recorded action potentials at compressed time scale.

also involved in egg-laying behavior. [10] The connective tissue sheath enclosing the ganglia and nerve connectives of *Aplysia juliana* was about 200 to 300 μm in thickness, only half the size of that of *Aplysia kurodai*. The abdominal ganglion of *Aplysia juliana* also seemed to deviate in overall structure from the prototype ganglia of *Aplysia kurodai*. The paired bag cell clusteres of *Aplysia juliana* appeared to develop prominently, often reaching almost the size of the hemiganglia. The bursting activity of a neuron in *Aplysia juliana* recorded at the neurobiophysics laboratory in Cheju National University was shown in FIG.1.

V. MODELS

All living cells are enclosed by a thin membrane, which is made up of phospholipid and protein molecules. The phospholipids provide the basic structure of the membrane and the proteins carry out specific functions. Embedded in the phospholipid bilayer are many different types of protein molecules. The ability of proteins to control the flow of ions is the underlying reason for the electrical activity exhibited by many types of cells. The driving force for ionic movement through open channels stems from the differences in the electric potential and the ionic concentrations across the membrane. The membrane potential is the voltage difference that exists across all biological membranes. It arises from an imbalance of electrical charges across the membrane, as well as ionic current flow through the membrane. Thus, there are two forces acting on any ion, namely an electrostatic force due to the membrane potential and a diffusional force due to the concentration differences.

In particular, the membrane can be thought of as a leaky capacitor. The membrane current i_m thus is the sum of the capacitive current and all ionic currents, viz.,

$$i_m = C_m \frac{dV}{dt} + \sum I_{ions}, \qquad (1)$$

where C_m is more-or-less constant specific capacitance of the membrane, V is the membrane potential, t is the time, and $\sum I_{ions}$ is the sum of all ionic currents, depending on the types of channels present in the membrane.

Normally, i_m is zero, due to Kirchhoff's Law, which essentially restates the law of conservation for charge. That is, the capacitive and ionic currents are in balance,

$$C_m \frac{dV}{dt} = -\sum I_{ions}. \qquad (2)$$

The above expression forms the starting point for all mathematical models of membrane electrical activity following the Hodgkin-Huxley modeling theory. An important assumption is that all ionic currents flow independently of each other.

In particular, by Ohm's Law,

$$I_{ion} = \frac{V - V_{ion}}{R_{ion}}, \quad (3)$$

where R_{ion} is the resistance of membrane to the ion. However, instead of resistence, physiologists prefer to use conductance, which is the reciprocal of resistance. Defining the conductance of the ion, g_{ion}, to be

$$g_{ion} = \frac{1}{R_{ion}}, \quad (4)$$

equation (3) becomes

$$I_{ion} = g_{ion}(V - V_{ion}). \quad (5)$$

The conductance g_{ion} in effect measures the permeability of the membrane to the ion.

VI. THE PLANT MODEL

The R-15 pacemaker neuron of *Aplysia* fires membrane action potentials in bursts, and perhaps it is the most widely-studied bursting pacemaker. Although a number of Hodgkin-Huxley equivalent circuit models of R-15 have been developed, the form studied here is taken from Plant's paper.[5]

Following the scheme introduced by Hodgkin and Huxley, the conductance of the voltage-gated Na^+, and K^+ channel is written as

$$g_{Na} = \bar{g}_{Na} m_\infty^3 \, h \, , \quad (6)$$

$$g_K = \bar{g}_K n^4, \quad (7)$$

where $\bar{g}_{Na}$, $\bar{g}_K$ are the maximum conductance of the channels and m_∞ is the voltage dependency of the steady-state function, h is inactivation parameter, and n^4 is the fraction of K^+ activation. Similarly, the conductance of the voltage-gated Ca^{2+} channel is written as

$$g_{Ca} = \bar{g}_{Ca} \, x \, , \quad (8)$$

where a slowly activating conductance, x, may include sodium and calcium. The conductance for the Ca^{2+}- activated K^+ channel is written by Plant as

$$g_{K-Ca} = \bar{g}_{K-Ca} \frac{Ca/K_d}{1 + Ca/K_d}, \quad (9)$$

where $\bar{g}_{K-Ca}$ is the maximum conductance of the channel, Ca is the intracellular calcium concentration, and K_d is the dissociation constant for Ca^{2+} bound to channel gate.

The flow of other ions is reflected in a leakage current of non-specific nature. The leakage current is assumed to have a constant, relatively small, conductance g_L.

Based on equations (5) - (9), the ionic currents are

$$I_{Na}(V) = \bar{g}_{Na} m_\infty^3 \, h \, (V - V_{Na}), \quad (10)$$

$$I_K(V) = \bar{g}_K \, n^4 \, (V - V_K), \quad (11)$$

$$I_{Ca}(V) = \bar{g}_{Ca} \, x \, (V - V_{Ca}), \quad (12)$$

$$I_{K-Ca}(V) = \bar{g}_{K-Ca} \frac{Ca/K_d}{1 + Ca/K_d} \, (V - V_K), \quad (13)$$

$$I_L(V) = \bar{g}_L(V - V_L), \quad (14)$$

where $I_{Na}, I_K, I_{Ca}, I_{K-Ca}, I_L$ are the currents flowing through the voltage-gated Na^+, Ca^{2+}, and K^+ channels, the Ca^{2+}-activated K^+ channel, and the leakage channel respectively. V_{Na}, V_K, V_{Ca}, and V_L are the Nernst potentials for sodium, potassium, calcium, and the leakage respectively.

From equation (2), the rate of change for the membrane potential V then satisfies

$$C_m \frac{dV}{dt} = -[I_{Na}(V) + I_K(V) + I_{Ca}(V) + I_{K-Ca}(V) + I_L(V)], \quad (15)$$

The inactivation and activation variables h, n, and x satisfy the relaxation equations introduced by Hodgkin and Huxley, namely,

$$\frac{dh}{dt} = \frac{h_\infty(V) - h}{\tau_h(V)}, \quad (16)$$

$$\frac{dn}{dt} = \frac{n_\infty(V) - n}{\tau_n(V)}, \quad (17)$$

$$\frac{dx}{dt} = \frac{x_\infty(V) - x}{\tau_x}, \quad (18)$$

The voltage dependencies of the steady-state functions h_∞, and n_∞, and the functions τ_h, τ_n corresponding to the time constants have exactly the same form as in Hodgkin and Huxley model. However, because of the proposed importance of the change in the intracellular calcium concentration, a fifth equation is required. The equation for Ca thus is

$$\frac{dCa}{dt} = \rho\,[K_c\, x\, (V_{ca} - V) - Ca], \quad (19)$$

The variable Ca represents the calcium ion concentration at the inner face of the membrane. It is increased by inward calcium current at a rate $\rho\ K_c\ x\ (V_{ca} - V)$ where V_{Ca} is the equilibrium potential for calcium(assumed constant), and it is decreased at a rate $\rho\ Ca$.

The definition of the steady-state functions $m_\infty, h_\infty, n_\infty$ and x_∞ and the functions $\tau_h(V), \tau_n(V)$ complete the description of the Plant model. They are

$$y_\infty(\bar{V}) = \frac{\alpha_y(\bar{V})}{\alpha_y(\bar{V}) + \beta_y(\bar{V})}, \quad (20)$$

$$\tau_z(\bar{V}) = \frac{3.8}{\alpha_z(\bar{V}) + \beta_z(\bar{V})}, \quad (21)$$

for $y = m,\ h,n$, and $z = h,\ n$, where

$$\alpha_m(V) = 0.1\frac{50 - V}{e^{\frac{50-V}{10}} - 1}, \quad (22)$$

$$\beta_m(V) = 4e^{\frac{25-V}{18}}, \quad (23)$$

$$\alpha_h(V) = 0.07e^{\frac{25-V}{20}}, \quad (24)$$

$$\beta_h(V) = \frac{1}{e^{\frac{55-V}{10}} + 1}, \quad (25)$$

$$\alpha_n(V) = 0.01\frac{55 - V}{e^{\frac{55-V}{8}} - 1}, \quad (26)$$

$$\beta_n(V) = 0.125e^{\frac{45-V}{90}}, \quad (27)$$

$$x_\infty(V) = \frac{1}{e^{A(B-V)} + 1}. \quad (28)$$

Here $\alpha_y(V)$, $\beta_y(V)$ $(y = m,\ h,\ n)$ are activation time constants and inactivation time constant respectively. Moreover $\bar{V} = \frac{127}{105}V + \frac{8265}{105} = 1.21V + 78.71$, and unit's of α's, and β's are $\frac{m}{s}$.

VII. RINZEL AND LEE'S FAST AND SLOW PROCESSES

Without question, Ca is the slowest variable while V, h, and n are substantially faster than x. Based on these comparisons we iden-

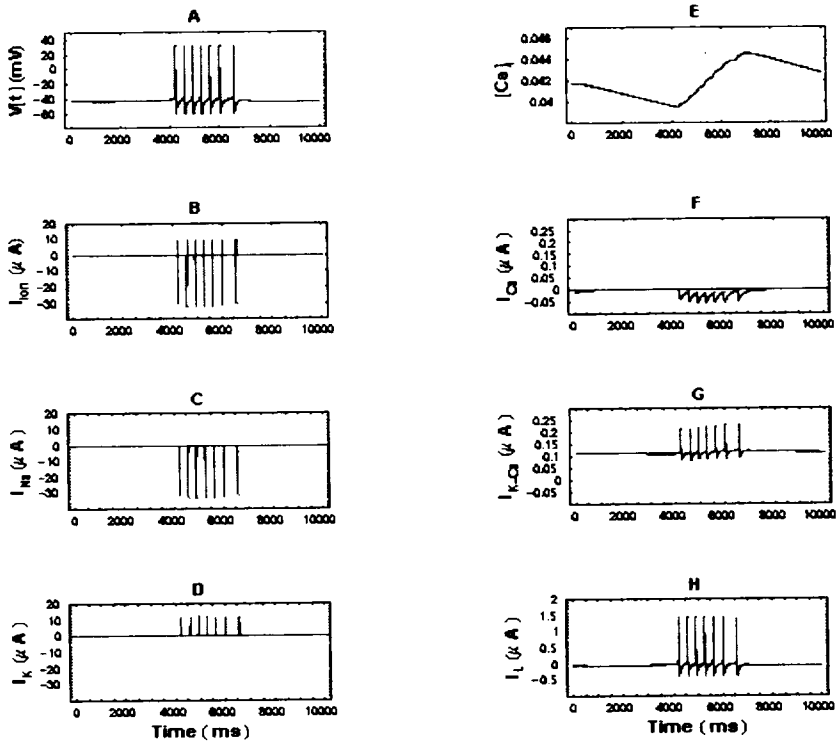

FIG. 2: Membrane currents contributing to the electrical activity. A: Left top panel illustrates a burst generated by the Rinzel and Lee's model with the parameters represented in section V. B,C,D: the total ionic current I_{ion}, fast inward Na^+ current I_{Na}, delayed rectifier current I_K contributing to the spikes during a burst are plotted respectively below the membrane potential on the same time scale. E: Corresponding level of Ca are shown in the right top panel. F, G, H:The slow inward Ca^{2+} current I_{Ca}, the outward Ca^{2+}-activated K^+ current I_{K-Ca}, and the leakage current I_L are illustrated respectively below it.

tify the fast subsystem (FAST) as

$$\begin{aligned} C_m \frac{dV}{dt} &= -I_{ion}(V,h,n;x,Ca) \\ &= -\bar{g}_{Na}\, m_\infty^3 h(V - V_{Na}) \\ &\quad -\bar{g}_{Ca}\, x\, (V - V_{Ca}) \\ &\quad -(\, \bar{g}_K\, n^4 + \bar{g}_{K-Ca}\, \frac{Ca}{0.8 + Ca}) \,(V - V_K) \\ &\quad -\bar{g}_L(V - V_L), \end{aligned} \tag{29}$$

$$\frac{dh}{dt} = \frac{h_\infty(V) - h}{\tau_h(V)}\,, \tag{30}$$

$$\frac{dn}{dt} = \frac{n_\infty(V) - n}{\tau_n(V)}\,, \tag{31}$$

in which x and Ca are treated as parameters. The slow subsystems (SLOW) is

$$\frac{dx}{dt} = \frac{x_\infty(V) - x}{\tau_x}\,, \tag{32}$$

$$\frac{dCa}{dt} = \rho\ [\ K_C\ x\ (V_{Ca} - V) - Ca\ ]. \quad (33)$$

where $V = V(t; x, Ca)$ is an attracting solution of Eqs. (29)-(31).[8]

The key idea in Rinzel's treatment of the system is to identify a fast and a slow subsystem. Due to the smallness of the ρ in Eq.(33), the time course of Ca is much slower than that of the remaining variables, V and n. In fact, the dynamics of Ca determine the time scale of the slow overall periodic behavior. [11]

A common feature of these model is that bursting cells have an inward current (which depolarizes the membrane) and a competing outward current (which hyperpolarizes the membrane). These competing currents are the basic components of the spikes during the active phase. There is also an outward "pacemaker" current which, is modulated by activation of Ca-dependent K-channels. The termination of the spike train, thus, is due to the activation of a calcium-dependent outward potassium current, and this activation switches the membrane to hyperpolarization. [3]

The model has a slowley activating conductance, x, for inward current which, in general, may include sodium and calcium. The accumulation of calcium during the burst turns on g_{K-Ca} (an outward current) which counteracts the slow inward current. During the interburst or silent phase, this conductance decays as calcium is removed. The consequenct slow depolarization eventually leads to reactivation of the slow V-dependent inward current, onset of the active phase, and thus to activation of the rapid, spike-generating currents.[8]

There is evidence that the termination of the bursts, and the interburst hyperpolarization that follows, are the results of an increase in the intracellular Ca^{2+} ionic concentration. The increase in $[Ca^{2+}]_i$ is brought about by the action of the voltage-gated Ca^{2+} channels during the burst of spikes. Calcium entry through this channel is vital to diverse neuronal functions such as transmitter release, spike initiation, and rhymic firing. [3]

VIII. SIMULATION OF THE BURSTING ACTIVITY OF A NEURON IN *Aplysia juliana*

The values of all parameters we used in this simulation are as follows:

$C_m = 1\mu F/cm^2$, $V_{Na} = 42mV$,
$V_{Ca} = 150mV$, $V_K = -120mV$,
$V_L = -40mV$, $\bar{g}_{Na} = 4.0mmho/cm^2$,
$\bar{g}_{Ca} = 0.0061mmho/cm^2$,
$\bar{g}_K = 0.5mmho/cm^2$,
$\bar{g}_{K-Ca} = 0.03mmho/cm^2$,
$\bar{g}_L = 0.02mmho/cm^2$, $\rho = 0.0000149\frac{m}{s}$,
$K_c = 0.0399\frac{m}{V}$,
$A = 0.9$, $B = -2$, $\tau_d = 255$.

Membrane currents contributing to the electrical activity during a typical burst was shown in FIG.2. Left top panel of FIG.2 illustrates a burst generated with the parameters shown just before. The the fast inward current I_{Na}, the delayed rectifying K^+ current I_K, the slow inward Ca^{2+} current I_{Ca}, the Ca^{2+}-activated K^+ current I_{K-Ca}, and the leak current I_L contributing to the spikes during a burst are plotted below the membrane potential on the same time scale.

Once the bifurcation structure of the fast subsystem is understood, the dynamics of Ca are included in order to account for the overall bursting behavior. The first step in the bifurcation analysis is to determine the steady states. We require,

$$\begin{aligned} & I_{SS}(V; Ca) \\ = & \bar{g}_{Na}\ m_\infty{}^3 h_\infty(V)(V - V_{Na}) \\ & + \bar{g}_{Ca}\ x_\infty\ (V - V_{Ca}) \\ & + [\ \bar{g}_K\ n\infty^4 + \bar{g}_{K-Ca}\ \frac{Ca}{0.8 + Ca}\ (V - V_K) \\ & + \bar{g}_L(V - V_L) \\ = & \ 0. \end{aligned} \quad (34)$$

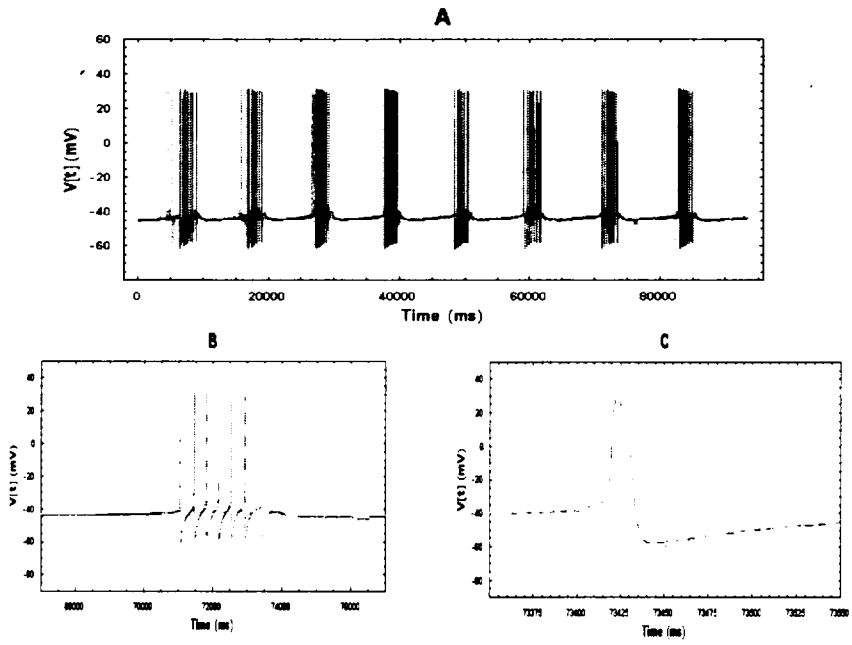

FIG. 3: A. Comparison of an action potential recorded from the exemplar cell(the dark one) and a simulated action potential (the light one). B. The solid curves are the simulated action potentials obtained fromed the Rinzel and Lee's model and the dasded curves are the recorded action potentials for comparison of mambrane voltage behavior between action potentials.

Note that we denote Ca as a parameter in I_{SS} by use of the semicolon.

Fig.4A,B,C show the behavior of I_{SS} as a function of V for several biophysical values of $\bar{g}_{Na}, \bar{g}_{K-Ca}$, and Ca respectively. Fig.4D also shows that there is one steady state ($I_{SS} = 0$) at high value of V. Similarly, for lower values of V, there are three and four steady states. [11]

IX. DISCUSSION

For the evaluation and algebraic manipulation of analytic prescriptions, many modelers have used symbol manipulation program like Mathematica and Maple with success. [12]

In this paper, using Mathematica program, we have simulated the bursting activity of neuron R15 in *Aplysia juliana* recorded at the Neurobiophysics laboratory in CNU. The Rinzel and Lee's model based on the Plant's model was use to simulate the activity of R15. Although the recorded and simulated results did not coincided exactly, we saw the possibility to have better results in the near future. Membrane currents and Steady-State I-V relationships contributing to the electrical activity will be analyzed.

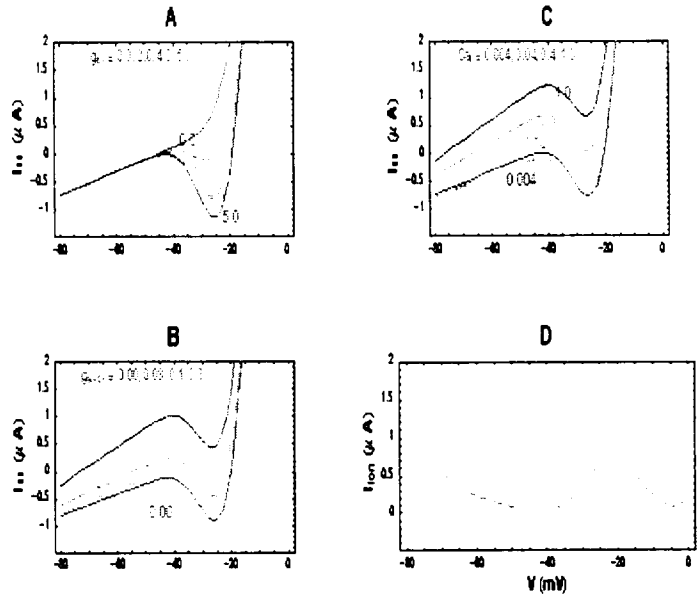

FIG. 4: A: I_{SS} as a function of V for $\bar{g}_{Na}$= 0.0, 2.0, 3.0, and 4.0. B: I_{SS} as a function of V for $\bar{g}_{K-Ca}$= 0.0, 0.03, 0.1, and 0.3. C: I_{SS} as a function of V for Ca= 0.004, 0.04, 0.4, and 1.0. D: Curve of steady states of the fast subsystem.

[1] Richard E. Plant, and M. Kim, " On the Mechanism Underlying Bursting in the *Aplysia* Abdominal Ganglion R15 Cell", Mathematical biosciences, **26**, 357-375 (1975).

[2] C. C. Canavier, J. W. Clark, and J. H. Byrne, " Simulation of the Bursting Activity of Neuron R15 in *Aplysia*: Role of Ionic Currents, Calcium Balence, and Modulatory Transmitters", Journal of Neurophysiology **66** (No.6), 2107-2124 (1991).

[3] Teresa Ree Chay, and Daniel L. Cook, " Endogeneous Bursting Patterns in Excitable Cells", Mathematical biosciences, **90**, 139-153 (1988).

[4] Richard E. Plant, and M. Kim, and M. Kim, " Mathematical Description of a Bursting pacemaker Neuron by a Modification of the Hodgkin-Huxley Equations", Biophysical Journal, **16**, 227-244 (1976).

[5] Richard E. Plant, " Bifurcation and Resonance in a Model for Bursting Nerve Cells", J. Math. Biology, **11**, 15-32 (1981).

[6] Teresa Ree Chay, " Eyring Rate Theory in Excitable Membranes: Application to Neuronal Oscillations", J. Phys. Chem. , **87** , 2935-2940 (1983).

[7] J. L. Hindmarsh, and R. M. Rose, " A Model of Neuronal bursting using three coupled first order differential equations", Proc. R. Soc. Lond. B**221**, 87-102 (1984).

[8] John Rinzel, and Young Seek Lee, " Dissection of a Model for neuronal parabolic bursting", J. Math. Biol., **25**, 653-675 (1987).

[9] S. S. Demir,R. J. Butera, Jr., A. A. DeFranceschi, J. W. Clark, Jr., and J. H. Byrne,"Phase Sensitivity and Entainment in a Modeled Bursting Neuron", Biophysical

Journal **72**, 579-594 (1997).

[10] Chae-Seok Lim, Do Yong Chung, and Bong-Kiun Kaang, " Partial Anatomical and Physiological Characterization and Dissociated Cell Culture of the Nervous System of the Marine Mollusc kurodai", Mol. Cells, **7** (No.3), 399-407 (1997).

[11] G. de Vries,"Analysis of models of bursting electrical activity in pancreatic beta cells", a doctoral dissertation, The University of British Columbia, 1995.

[12] J. Rinzel, and G. B. Ermentrout, "Analysis of neural excitability and oscillations." In: C. Koch,and I Segev, eds. Methods in Neuronal Modeling: From Ions to Networks, (MIT Press, 1998), 251-291.